Published by :
http://www.ijert.org

International Journal of Engineering Research & Technology (IJERT)
ISSN: 2278-0181
Vol. 11 Issue 10, October-2022

LCLU Classification using SVM, MLC and ANN of Multispectral Imagery from Sentinel-2

Yash Khurana
School of Computer Science and Engineering
Vellore Institute of Technology
Vellore, 632014, India

Swamita Gupta
School of Computer Science and Engineering
Vellore Institute of Technology
Vellore, 632014, India

***Abstract*— Land Cover or Land Use (LCLU) classification is essential for a plethora of activities, including navigation, agriculture and urban planning. Remote Sensing (RS) imagery provides an efficient way of identifying various land classes through an aerial view when passed through a machine learning or deep learning classifier, also known as Land Cover Land Use (LCLU) Classification. This paper performs LCLU Classification on multispectral imagery obtained from the Sentinel-2 satellite using machine learning classifiers of Support Vector Machines (SVM), Maximum Likelihood Classifier (MLC) and Artificial Neural Networks (ANN) and is evaluated on the metrics of confusion matrices, Producer Accuracy (PAC), User Accuracy (UAC), Overall Accuracy (OAC) and Kappa Statistics. Experiments revealed that SVM significantly outperforms the architectures by reporting an OAC of 98.1% along with a 0.976 Kappa coefficient. Further, these results are analyzed to identify the knowledge gaps as well as the potential for future research.**

Keywords*— *Remote Sensing; SVM; ANN; MLC; LCLU Mapping; Sentinel-2

I. INTRODUCTION

Land Cover or Land Use (LCLU) represents the physical composition of Earth's surface area. It includes natural characteristics like forests and water bodies as well as human activity related elements of road networks and residential areas. It is responsible for the radiation balancing of the earth's surface and any changes in its pattern affects the environment and its processes both by a local and global scale. In addition to using the land for anthropogenic activities, humans rely on it to meet their fundamental requirements for food and shelter. This makes it crucial to identify and map the land cover for monitoring research, urban planning, and resource management because changes in the physical features of the land reflect the socio-economic, natural, and biological processes of a specific region [1]–[4]

There have been several research on sustainable development based on LCLU classification conducted in the past. Using the Random Forest (RF) approach for categorization, [5] makes an attempt to combine remote sensing data with social media data from twitter usage to assess urban expansion in Tanzania's Morogoro urban region from 2011 to 2017. [6] suggests an integrated GIS and remote sensing-based strategy to track and assess land development for the China's Pearl River Delta. [7] uses very high resolution (VHR) images to monitor LCLU change in Delhi's north-western districts to aid policymakers in controlling land development. Recent studies have analyzed and evaluated the changing patterns of urban landscapes and how they affect the land surface temperature in and around Delhi [8]–[10]. These studies show a warming tendency throughout the course of the research periods, which makes it necessary to analyze Land Cover changes to offset the consequences of rising urbanization.

While very high resolution (VHR) optical satellites capture imagery with a sub-meter pixel resolution, it is subject to high image cost, relief displacement and shadowing effect. This creates the necessity of a strong and robust architecture which can optimally perform LCLU classification without precise high-resolution data. This research assesses high performing machine learning classifiers of Support Vector Machines (SVM), Maximum Likelihood Classifier (MLC), and Artificial Neural Networks (ANN) for the task of LCLU classification on medium resolution multi-spectral imagery. These classifiers are analyzed using the metrics of confusion matrices, Producer Accuracy (PAC), User Accuracy (UAC), Overall Accuracy (OAC), and Kappa Statistics Coefficient. The knowledge gaps and the possibility for further study are also determined by further analysis of these data.

The remainder of this work is structured as follows. The advancements achieved in the discipline are discussed and analyzed in Section II. In Section III, we go over our suggested approach and classifiers. The dataset and experimental set-up for the proposed investigation are described in Section IV. The analysis of the experiments' outcomes is reported in Section V. Section IV wraps up the paper by summarizing the work done.

II. LITERATURE REVIEW

Assessments of LCLU classification maps give meaningful and relevant information about the landscape of any area and have been utilized for understanding a region and for making both geographic and administrative decisions. These maps are produced using a variety of machine learning and deep learning techniques. These algorithms may be divided into six main groups.

A. Pixel based Approaches

The class of each individual pixel in the picture is identified independently using per-pixel techniques. This is accomplished by using the spectral data of the pixel to compare the n-dimensional feature vector of each pixel to the prototype vector of each class. Per-pixel techniques ignore the contributions of many pixels that make up a class by assuming that each pixel only belongs to one class. Techniques for classifying individual pixels may be parametric or non-parametric. The typical assumptions made by parametric classifiers are that the data set is normally distributed and that the class density functions are known beforehand. They become quicker, simpler, and use less data as a result. A regularly distributed dataset, however, is

International Journal of Engineering Research & Technology (IJERT)
ISSN: 2278-0181
Vol. 11 Issue 10, October-2022

uncommon in the actual world. As a result, the assumption of a normal spectral distribution is frequently broken when working with complicated landscapes. The limited structure of these methods, which sometimes makes it extremely difficult to combine spectral data with auxiliary data, is another significant problem. The Maximum Likelihood Classifier is the most often used parametric technique because of its dependability and simplicity. Non-parametric classifiers do not require additional statistical parameters like the mean vector or covariance matrix and do not presume that the data is regularly distributed. This makes it far more applicable to situations in the real world. Numerous studies in this area have shown that non-parametric classifiers produce results that are far superior than those produced by parametric ones [11]. The most popular non-parametric classifiers are Artificial Neural Networks (ANNs), which include models like Convolutional Neural Networks (CNNs , Hopfield Neural Networks [12]–[15] and Granular Neural Networks [16], [17], Support Vector Machines (SVMs) - used in many forms such as, Active SVM Learning [18]–[20], Semi-supervised SVM Learning [21]–[24] and SVM integrated with other approaches [25]–[29], Decision Trees (DTs) [30]–[32] and expert systems.

B. Sub-pixel based Approaches

The majority of conventional classification techniques rely on per-pixel methods, in which each pixel is assigned to a single category, with the land-cover classes being mutually exclusive. Mixed pixels are, nonetheless, a fairly typical occurrence due to the diversity of real-world landscapes, particularly in the case of medium or low-resolution data. The existence of mixed pixels creates a major challenge when using this data for activities like mapping tiny agricultural farms in heterogeneous settings. In order to overcome this mixed pixel problem, sub-pixel techniques were created, which work by calculating the fractional percentage of each form of land cover in a pixel on the basis of an acceptable training dataset. One of the most well-liked sub-pixel-based methods is called SMA (Spectral Mixture Analysis), and it compares the spectral signatures of the various forms of land cover in a pixel to a set of endmember spectra to calculate the fractional proportions of each pixel. One of the most important SMA phases is endmember selection. Various forms of this have been used in earlier research, including [33]–[35] Earlier studies have demonstrated how SMA can increase classification accuracy compared to other approaches, particularly when dealing with low- or medium-resolution data [36], [37]. Subpixel categorization has a number of problems, including a challenge in determining accuracy. However, research that are proposing novel methodologies for accuracy evaluation have recently come to light [38]. The Fuzzy based methodology is another pixel-based method for resolving the mixed pixel problem. In a fuzzy representation, it was conceivable for one region to include numerous, incomplete members of every potential land cover class. Fuzzy-based strategies have been used in a number of approaches. In contrast to current state-of-the-art techniques, [39] presents a large-scale remote sensing picture segmentation approach that integrates fuzzy area competition with the Gaussian mixture model. Based on the collected indices from MODIS data, [40] uses a Fuzzy C-Means Clustering Algorithm to divide 38 watersheds into three homogenous groups. Other approaches to subpixel classification include using neural networks [41], SVM-based classification [42], and adaptive sparse subpixel mapping [43].

C. Object based Approaches

The idea of numerous pixels constituting a land cover class is ignored by pixel-based classification approaches, which presume that each picture pixel is a separate land cover class. This can be a serious danger to the categorization accuracy when working with high- and very high-resolution photography. Using a segmentation algorithm, object-based classification approaches first divide the image pixels into spectrally similar-looking picture objects before classifying those objects individually, as opposed to classifying individual pixels, as is the case with pixel-based classification techniques. These methods now yield superior outcomes when working with images with precise spatial resolution. The object-based categorization strategy, on the other hand, has its own set of restrictions regarding over- and under-segmentation [44]. The first is that under-segmentations result to image objects that end concealing more than land cover class and thus introduce errors in classification. Further, the features extracted from these incorrectly segmented image objects owing to over- or under-segmentation will not actually reflect shape and area of the real world and might end up lowering the overall classification accuracy. The eCognition approach, which has shown to be adaptable and extremely accurate [45], is one of the most widely utilized techniques today.

D. Knowledge based Approaches

Road networks, soil maps, housing and population densities, and other types of auxiliary data are becoming more widely accessible and may be merged with the current categorization systems to improve accuracy. Making a knowledge-based classifier using the selected auxiliary data and the geographical distribution pattern of land-cover classes is one technique to do this. F or instance, data on population, housing, road density, and industrial land areas may aid to improve overall classification accuracy when dealing with urban land cover land use (ULCLU) categorization. Three approaches are put forth by [46] for developing rules for categorizing images: (1) explicitly eliciting knowledge and rules from experts, then refining the rules; (2) using cognitive methods to implicitly extract variables and rules; and (3) empirically generating rules from the observed data using automatic induction techniques. The capacity of the knowledge-based categorization strategy to include data from many sources has helped it become quite popular in recent years. [47] suggests a classifier that divides the scene's L- and C-Band polarimetric SAR readings into four categories: tall vegetation (trees), short vegetation, urban, bare surface, or last category (includes water surfaces, bare soil surfaces, and concrete or asphalt-covered surfaces). The classifier is built in a way that it sequentially constructs the relevant discriminators using information about the characteristics of radar backscattering from surfaces and objects. For all situations and categories, the accuracy ranged from 91 to 100%. A knowledge-based approach is suggested in [48] for integrating readily available spatial context data from a GIS with remotely sensed image processing. Both the picture and the geographical context rules are contained in the knowledge base. Using the Dempster-Shafer paradigm of evidential reasoning,

International Journal of Engineering Research & Technology (IJERT)
ISSN: 2278-0181
Vol. 11 Issue 10, October-2022

probabilistic data from the rule base and the image classifier are integrated. [49], [50] are two other papers that make use of knowledge-based classifiers.

E. Spatio-Contextual based Approaches

Although conceptual simplicity and low cost of computing are two of the many benefits of spectral classifiers, their drawbacks are also readily apparent [51]. The total classification accuracy of spectral-only classifiers is reduced because only a limited number of land cover classes may be successfully distinguished using spectral information. Spatio-contextual classifiers make use of the spatial information shared by nearby pixels to increase their overall classification accuracy. Spatio-contextual analysis techniques can be classified into three methodological approaches [52]: Text extraction, MRF models and Spatio-contextual with object-based image analysis.

F. Combined Approaches

Each classifier has a unique set of benefits and drawbacks. For instance, if a normally distributed dataset and representative statistical parameters (such as the mean vector and covariance matrix) were constructed from the training samples, a parametric classifier like MLC would produce excellent results. However, non-parametric classifiers like neural networks and decision trees will perform better when the picture data are not typically disturbed. Earlier studies have frequently shown that combining two or more of these classifiers can produce much superior results. Findings from [53] demonstrate that multi-classifier systems may successfully increase the stability and accuracy of remote sensing image classification, and that diversity measures play a significant role in the integration of multiple classifiers. The survey also offers a direction for further study and approaches for algorithm improvement. [54] indicates that as compared to the output of a univariate decision tree classifier, all ensemble decision tree techniques enhance overall classification accuracy by roughly 4%. The creation of a set of guidelines for merging the results from various classifiers is the most crucial stage in creating a multi-classifier system. [55] examines several approaches for combining multiple categorization results, including production rules, sum rules, stacked regression techniques, and more.

Over the years, a number of categorization algorithms and methods have been created, however no single approach is effective for all jobs. Per-pixel, sub-pixel, object-based, knowledge-based, spatio-contextual-based, and multi-classifier systems are some of the several types of classification methods. In the modern world, per-pixel categorization is the most popular. However, because there are mixed-pixels, its precision might not always be sufficient. In particular for low- and medium-resolution imaging, subpixel-based techniques can achieve improved accuracy by resolving the mixed-pixel issue. Spatio-contextual classifiers handle the issue of within-class spectral variability and the spatial dependence of the pixels in high-resolution imaging, even though the issue of mixed pixels may be less of an issue. Knowledge-based classifiers are preferable to others when working with data from numerous sources, including ancillary data, together with sophisticated non-parametric classifiers as neural networks and decision trees. A group of classifiers can be used in multi-classifier systems to overcome the constraints of each one separately. To find the optimal sort of approach for a specific assignment, a comparison study of several categorization techniques is frequently carried out [56]–[58]. It has repeatedly been demonstrated that classifiers like MLC perform worse than contextual-based classifiers as well as non-parametric classifiers that utilize machine learning and SVM, with some small trade-offs in total classification accuracy and processing time.

III. METHODOLOGY

This section describes the methodology used for LCLU classification as demonstrated in Fig 1. It can be further broken down into the following parts.

A. Preprocessing Satellite Imagery

A satellite's multispectral imaging sensors frequently record various spectral bands, each of which has a distinct function. The noise created by optical sensors has a calibration mistake or is an inherent feature of the hardware in these bands, which are acquired from satellites. Noise can also result from atmospheric influences like cloud cover, topography impacts, or even shadows. The performance of ULCLU Classification is hampered by this noise. Remote sensing data preprocessing typically consists of two main steps: (A) Radiometric calibration; (B) Atmospheric and geometric distortion correction. Additionally, other mistakes such line drops and striping are eliminated.

B. LCLU Classification

SVM, MLC and ANN models were utilized for this investigation, that were trained and assessed on the same. The optimum hyperparameters for each baseline model are identified using K-Cross Validation, where K is set to 5. The fundamentals of the baseline models and the best hyperparameter choices are covered in the next subsections.

1) SVM

SVM uses a kernel to transform a complicated non-linear space into a linear one. This kernel may be sigmoid, radial basis function (RBF), polynomial, linear, or polynomial. SVM seeks to solve the maximizing issue of a convex function to discover the best hyperplane that fits through the training data classes. The best hyperplane for the n-dimensional job is discovered by an iterative procedure for the training data, and it is then applied to the evaluation data. The linear function used in this investigation offered the best overall accuracy while also requiring the least amount of training time. The radial function's gamma was set to 0.333, and the punishment parameter was set to 100.00 after a number of trials.

2) MLC

In a parametric technique, the distribution of pixel values across different classes is predicated on a posterior probability. Using a learning function inferred from the training data, the classifier then determines the probability that each pixel corresponds to each category of land cover. The following definition applies to the posterior probability of a class r_N:

$$P(r|\alpha) = \frac{P(r).P(\alpha|r)}{\sum_{j=1}^{N} P(j).P(\alpha|j)} \quad (1)$$

The probability threshold is set at 0.13%, and P(r) is the predetermined probability of any class r. N denotes the total

International Journal of Engineering Research & Technology (IJERT)
ISSN: 2278-0181
Vol. 11 Issue 10, October-2022

number of classes. P(α |r) denotes the conditional probability of α from any class r.

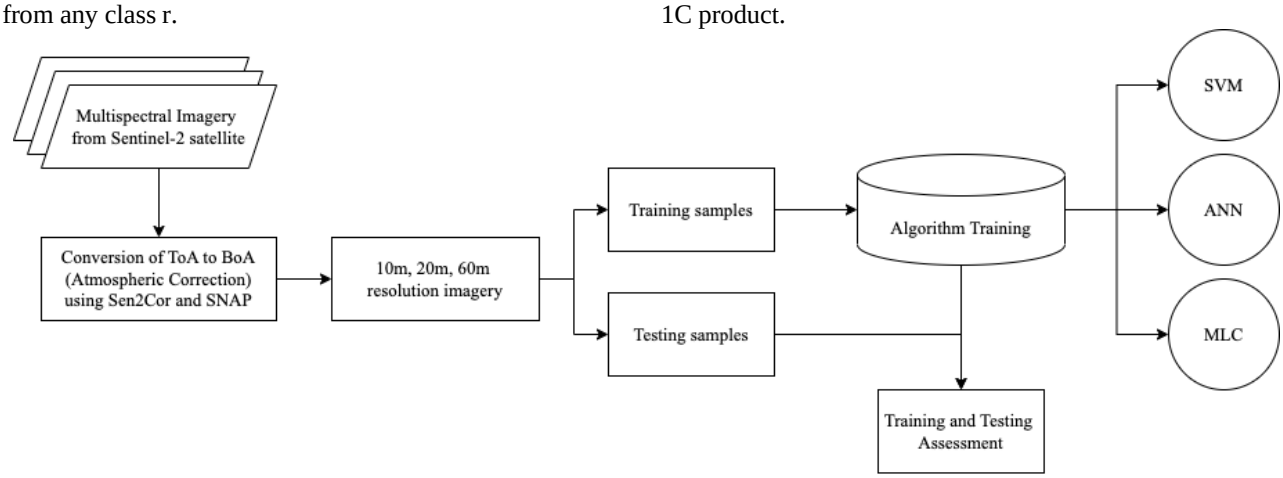

Fig 1. Flowchart of the implemented methodology

3) ANN

For the objectives of this study, multispectral footage from Sentinel-2 is classified using a feed-forward neural network with one hidden layer based on the backpropagation method. A gradient descent algorithm, the backpropagation method seeks to minimize loss between the input training samples and the output class. The learning rate is then used to update the backward weights once this defect in the pair has repeatedly been transported backward from the output layer to the input layer. The hyperparameters of the ANN are chosen after thorough scrutiny and multiple training and testing cycles in order to attain the maximum accuracy achievable. A sigmoid activation with a momentum rate of 0.9 and a learning rate of 0.2 is used in the neural network with one hidden layer during training, which lasts for more than 1000 iterations.

IV. EXPERIMENTAL SETUP

This section describes technical details of the experimental analysis conducted on the selected classification models.

A. Study Area

The study area is a 20 km x 20 km diversified topography as shown in Fig 2. It is situated in the south-west part of Pune in Maharashtra, India. At a height of 560 meters (1,840 feet) above sea level, Pune is located on the western edge of the Deccan plateau. It is located on the leeward side of the mountain range known as the Sahyadri, which serves as a barrier between it and the Arabian Sea. The average temperature of Pune, India, is between 20 and 28 °C (68 and 82 °F), which is classified as having a tropical wet and dry climate that is on the cusp of a hot semi-arid one. In the ten years between 1991 and 2001, the population of Pune, a significant industrial metropolis, massively increased.

B. Dataset

This work utilizes sentinel-2 imagery. Level 1-C imagery with tile ID of L1C_T43QCA_A026872_20220429T054147, acquired on 15th October 2022 from the USGS website [59], has been utilized here. This tile is made up of 100 km by 100 km, including our study area in the form of orthorectified tiles in the UTM/WGS 84 projection. Sentinel 2A product, which is utilized as data for this study, is created by preprocessing level 1C product.

Fig 2. Selected Study Area

C. Preprocessing Multispectral Imagery

The data from Sentinel-2 is given on the official USGS website as Level 1C data in the JPG2000 encoding/format. The Level 2A Algorithm (L2) is used to preprocess this data using the SNAP 7.0 toolbox and the Sen2Cor plugin (2.80). Scene Classification (SC) and Atmospheric Correction (S2AC) are the two components of the L2 algorithm; the former aims to provide a pixel classification map, while the latter converts TOA (Top of Atmosphere) reflectance into BOA (Bottom of Atmosphere) reflectance. Product 2A, the pre-final processing's output, consists of atmospherically adjusted imagery with the cartographic impact removed. The WGS 84 UTM coordinate system is used to geo-reference this item.

D. Training the model

A vast number of samples are needed for supervised algorithm training, and these samples are crucial to the algorithm's ultimate quality, which is frequently defined by its

International Journal of Engineering Research & Technology (IJERT)
ISSN: 2278-0181
Vol. 11 Issue 10, October-2022

accuracy. Thematic maps can be used to pick training data. Though dependable and precise, such data may nevertheless contain inherent mistakes from earlier ULCLU classifications. This study employs training and validation data that were collected from true-color composite images of Sentinel-2 by matching with VHR imagery of Google Earth in order to prevent such discrepancies. In order to ensure the independence of the training and test samples, a 15m buffer is applied to each data point. Five ULCLU classes—barren terrain, residential areas/buildings, aquatic bodies, and road networks—are chosen for categorization purposes since the research region is part of an urbanized zone with uneven landscapes. The class-wise data samples for training and testing are further described in Table I.

Table I. Class-wise data samples for training and testing

	Training Points	Testing Points
Barren terrain	521	200
Residential area	600	200
Water bodies	463	200
Vegetation	499	200
Road Network	511	200

V. RESULTS AND DISCUSSION

This section discusses and evaluates the experimental results obtained by the selected classification models.

A. Performance Metrics

Precision and recall are the two most often used qualitative criteria for rating binary classification algorithms. These factors are frequently referred to as User's accuracy and Producer's accuracy in remote sensing. In addition, this study also uses Kappa Coefficient and Overall accuracy as assessment metrics. The ground truth and forecast images are cross-tabulated in the error matrices, from which all metrics are derived.

1) User's Accuracy (UAC)

The correctness of a map from the perspective of the user, not the map developer, is referred to as the user's accuracy. It informs us how often the class on the map will actually be present on the ground based and is synonymous to the term's precision and reliability. It is calculated as shown below.

$$UAC = \frac{TP}{TP + FP} * 100 \quad (2)$$

2) Producer's Accuracy (PAC)

Producer accuracy refers to the correctness of the map from the perspective of the map creator (the producer). This is the chance that a certain landscape of a region on the land is categorized as such or the frequency with which actual characteristics on the ground are accurately depicted on the classified map. The Omission Error's complement, the Producer's Accuracy, and recall are the same thing. The calculation is displayed below.

$$PAC = \frac{TP}{TP + FN} * 100 \quad (3)$$

3) Overall Accuracy (OAC)

The overall accuracy informs us what percentage of the reference locations were accurately mapped. In most cases, the total accuracy is given as a percentage, with 100% accuracy denoting a flawless classification in which all reference sites were properly categorized. The calculation is displayed below.

$$OAC = \frac{TP + TN}{TP + TN + FP + FN} * 100 \quad (4)$$

4) Kappa Statistic (k)

For qualitative items, the Cohen's kappa coefficient statistic is used to assess inter-rater reliability. Since it considers the potential that the agreement may have happened by chance, it is typically believed to provide a more reliable measurement than a simple % agreement estimate. For the observed accuracy P(A) and chance accuracy P(B), k can be calculated as shown.

$$k = \frac{P(A) - P(B)}{1 - P(B)} \quad (5)$$

B. Performance Analysis

In this study, the urban land cover is classified into five classes, namely barren terrain, residential area, water bodies, vegetation and road network. Out of all the implemented models, SVM reports the highest Overall Accuracy (OAC) of 98.1% and a Kappa Statistic measure of 0.976. The models MLC and ANN are also produced excellent results with an OAC of 96.4% and 95.6%, and with a Kappa Statistic measure of 0.955 and 0.945 respectively.

The classification results for SVM are statistically represented through its confusion matrix. Similarly, Table III showcases the confusion matrix for MLC and the results obtained from ANN are shown in Table IV.

TABLE II: Confusion Matrix for SVM

	Barren terrain	Residential area	Water bodies	Vegetation	Road Network
Barren terrain	193	0	0	1	0
Residential area	0	200	0	0	0
Water bodies	6	0	200	0	0
Vegetation	0	0	0	193	5
Road Network	1	0	0	6	195

TABLE III: Confusion Matrix for MLC

	Barren terrain	Residential area	Water bodies	Vegetation	Road Network
Barren terrain	190	1	0	1	0
Residential area	0	198	6	0	1
Water bodies	0	0	194	5	4
Vegetation	8	1	0	193	6
Road Network	2	0	0	1	189

TABLE IV: Confusion Matrix for ANN

	Barren terrain	Residential area	Water bodies	Vegetation	Road Network
Barren terrain	186	8	0	1	0
Residential area	2	191	1	1	1
Water bodies	12	0	199	1	4
Vegetation	0	1	0	189	4
Road Network	0	0	0	8	191

TABLE V: Class-wise Performance Evaluation

Model	Acc	Barren terrain	Residential area	Water bodies	Vegetation	Road Network
SVM	UAC	99.5%	100%	97.1%	97.5%	96.5%
	PAC	96.5%	100%	100%	96.5%	97.5%
MLC	UAC	98.9%	96.5%	95.5%	92.7%	98.4%
	PAC	95%	99%	97%	96.5%	94.5%
ANN	UAC	95.3%	97.4%	92.1%	97.4%	95.9%
	PAC	93%	95.5%	99.5%	94.5%	95.5%

International Journal of Engineering Research & Technology (IJERT)
ISSN: 2278-0181
Vol. 11 Issue 10, October-2022

TABLE VI: Overall Performance Evaluation

Model	Overall Accuracy	Kappa Statistic
SVM	98.1%	0.976
MLC	96.4%	0.955
ANN	95.6%	0.945

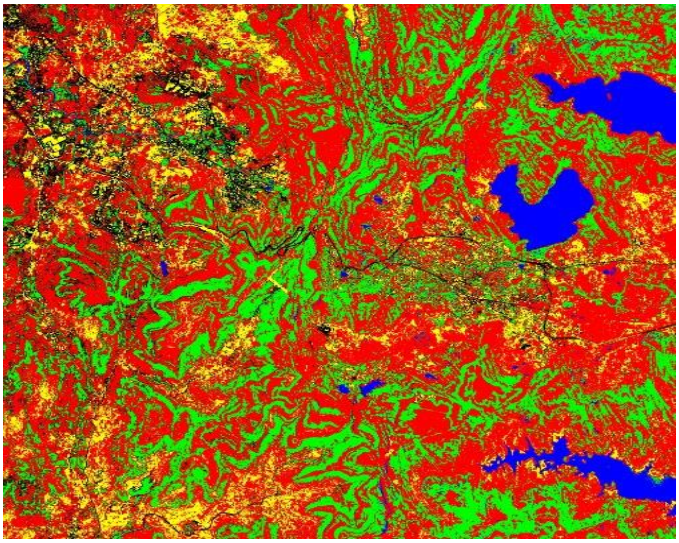

Fig 3. Classification map produced by SVM

The assessment of the three implemented models, with respect to the performance metrics User's Accuracy (UAC) and Producer's Accuracy (PAC) is elaborated for all land cover classes in Table V. While SVM showcases the best results among all the selected models, it reports the highest UAC and PAC for the class of residential area, followed by barren terrain. This is owing to the nature of the selected study area, which is an unevenly urbanized city located in a hilly region, causing a plethora of barren terrains in the area. Further, MLC is shown to outperform the other two models for the class of road networks, and can be further use for road identification and segmentation.

The overall performances of SVM, MLC and ANN are summarized in Table VI. Further, they are visualized as classification maps in Fig 3, Fig 4 and Fig 5 respectively, and provide further insight into the pixel-wise classification.

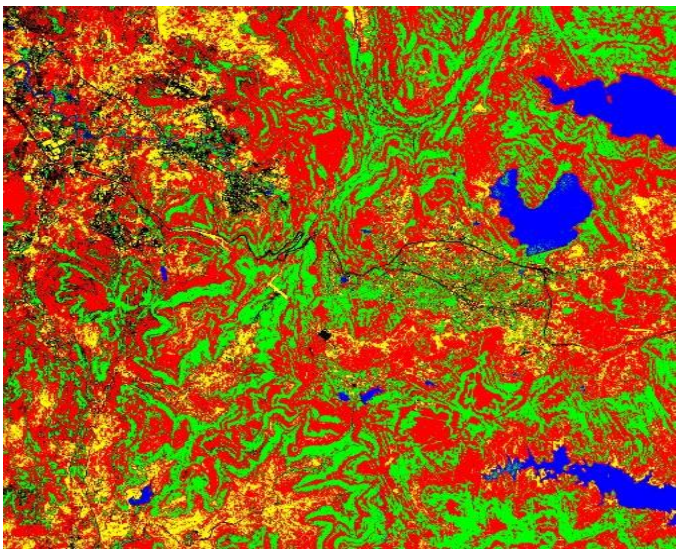

Fig 4. Classification map produced by MLC

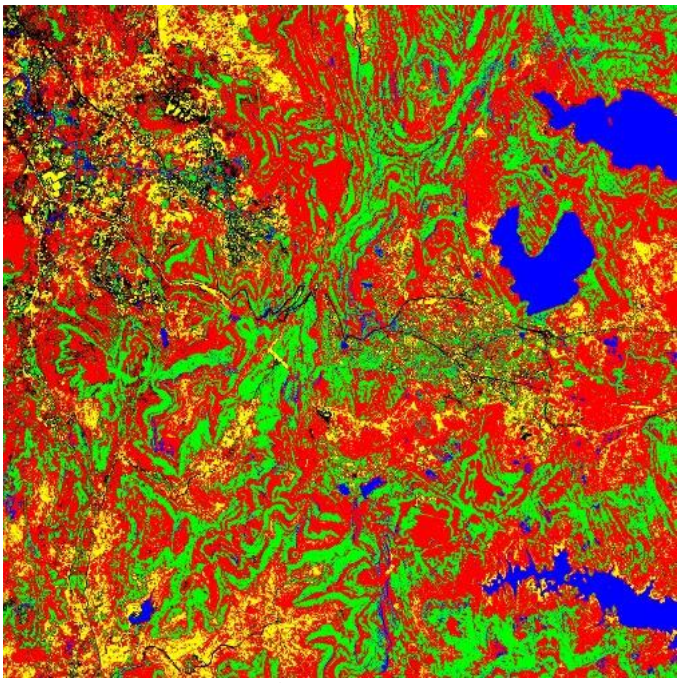

Fig 4. Classification map produced by ANN

VI. CONCLUSION

This work successfully classifies unevenly populated regions such as the hilly region of Pune, by using machine learning classifiers of SVM, MLC and ANN. With three red-edge bands, the Sentinel-2 mission offers a singular mix of data with various spatial resolutions, making it very appropriate for the categorization of ULCLU, as can be observed in this work. While all the models demonstrated outstanding results for the task of LCLU classification on multispectral imagery, SVM outperformed the others by reporting an overall accuracy of 98.1% and a 0.976 Kappa statistic. Further, preprocessing and atmospheric correction of raw satellite imagery aided in the high performance of the selected models by removing noise and unnecessary information from the images. This classification of Sentinel-2 imagery into the five classes of road networks, residential area, water bodies, road networks and barren terrain can be further utilized for various applications including navigation, sustainable development, urban planning and so on.

Future efforts may employ high- and very high-resolution imagery to improve accuracy and make more use of the classified LCLU maps. In order to increase accuracy, classification methods like convolutional networks and other sophisticated deep learning techniques can be used.

VII. REFERENCES

[1] B. Junge *et al.*, "Use of remote sensing and GIS for improved natural resources management: case study from different agroecological zones of West Africa," *http://dx.doi.org/10.1080/01431160903376415*, vol. 31, no. 23, pp. 6115–6141, 2010, doi: 10.1080/01431160903376415.

[2] M. M. Yagoub and G. R. Kolan, "Monitoring coastal zone land use and land cover changes of Abu Dhabi using remote sensing," *Journal of the Indian Society of Remote Sensing 2006 34:1*, vol. 34, no. 1, pp. 57–68, 2006, doi: 10.1007/BF02990747.

[3] M. K. Jat, P. K. Garg, and D. Khare, "Monitoring and modelling of urban sprawl using remote sensing and GIS techniques," *International Journal of Applied Earth Observation and*

International Journal of Engineering Research & Technology (IJERT)
ISSN: 2278-0181
Vol. 11 Issue 10, October-2022

Geoinformation, vol. 10, no. 1, pp. 26–43, Feb. 2008, doi: 10.1016/J.JAG.2007.04.002.

[4] K. Dhanaraj and D. P. Angadi, "Land use land cover mapping and monitoring urban growth using remote sensing and GIS techniques in Mangaluru, India," *GeoJournal 2020 87:2*, vol. 87, no. 2, pp. 1133–1159, Sep. 2020, doi: 10.1007/S10708-020-10302-4.

[5] A. Rahman, "Application of remote sensing and GIS technique for urban environmental management and sustainable development of Delhi, India," *Applied Remote Sensing for Urban Planning, Governance and Sustainability*, pp. 165–197, 2007, doi: 10.1007/978-3-540-68009-3_8/COVER.

[6] A. G. O. Yeh and X. Li, "An integrated remote sensing and GIS approach in the monitoring and evaluation of rapid urban growth for sustainable development in the Pearl River Delta, China," *http://dx.doi.org/10.1080/13563479708721678*, vol. 2, no. 2, pp. 193–210, 2007, doi: 10.1080/13563479708721678.

[7] A. Rahman, S. Kumar, S. Fazal, and M. A. Siddiqui, "Assessment of Land use/land cover Change in the North-West District of Delhi Using Remote Sensing and GIS Techniques," *Journal of the Indian Society of Remote Sensing 2012 40:4*, vol. 40, no. 4, pp. 689–697, Jan. 2012, doi: 10.1007/S12524-011-0165-4.

[8] B. Kumari *et al.*, "Satellite-Driven Land Surface Temperature (LST) Using Landsat 5, 7 (TM/ETM+ SLC) and Landsat 8 (OLI/TIRS) Data and Its Association with Built-Up and Green Cover Over Urban Delhi, India," *Remote Sensing in Earth Systems Sciences 2018 1:3*, vol. 1, no. 3, pp. 63–78, Nov. 2018, doi: 10.1007/S41976-018-0004-2.

[9] M. Panwar, A. Agarwal, and V. Devadas, "Analyzing land surface temperature trends using non-parametric approach: A case of Delhi, India," *Urban Clim*, vol. 24, pp. 19–25, Jun. 2018, doi: 10.1016/J.UCLIM.2018.01.003.

[10] D. Dutta, A. Rahman, S. K. Paul, and A. Kundu, "Changing pattern of urban landscape and its effect on land surface temperature in and around Delhi," *Environmental Monitoring and Assessment 2019 191:9*, vol. 191, no. 9, pp. 1–15, Aug. 2019, doi: 10.1007/S10661-019-7645-3.

[11] P. Verma, A. Raghubanshi, P. K. Srivastava, and A. S. Raghubanshi, "Appraisal of kappa-based metrics and disagreement indices of accuracy assessment for parametric and nonparametric techniques used in LULC classification and change detection," *Modeling Earth Systems and Environment 2020 6:2*, vol. 6, no. 2, pp. 1045–1059, Mar. 2020, doi: 10.1007/S40808-020-00740-X.

[12] X. Li, F. Ling, Y. Du, Q. Feng, and Y. Zhang, "A spatial–temporal Hopfield neural network approach for super-resolution land cover mapping with multi-temporal different resolution remotely sensed images," *ISPRS Journal of Photogrammetry and Remote Sensing*, vol. 93, pp. 76–87, Jul. 2014, doi: 10.1016/J.ISPRSJPRS.2014.03.013.

[13] A. J. Tatem, H. G. Lewis, P. M. Atkinson, and M. S. Nixon, "Increasing the spatial resolution of agricultural land cover maps using a Hopfield neural network," *http://dx.doi.org/10.1080/1365881031000135519*, vol. 17, no. 7, pp. 647–672, Oct. 2010, doi: 10.1080/1365881031000135519.

[14] A. J. Tatem, H. G. Lewis, P. M. Atkinson, and M. S. Nixon, "Super-resolution land cover pattern prediction using a Hopfield neural network," *Remote Sens Environ*, vol. 79, no. 1, pp. 1–14, Jan. 2002, doi: 10.1016/S0034-4257(01)00229-2.

[15] R. Sammouda, N. Adgaba, A. Touir, and A. Al-Ghamdi, "Agriculture satellite image segmentation using a modified artificial Hopfield neural network," *Comput Human Behav*, vol. 30, pp. 436–441, Jan. 2014, doi: 10.1016/J.CHB.2013.06.025.

[16] D. A. Kumar, S. K. Meher, and K. P. Kumari, "Adaptive granular neural networks for remote sensing image classification," *IEEE J Sel Top Appl Earth Obs Remote Sens*, vol. 11, no. 6, pp. 1848–1857, Jun. 2018, doi: 10.1109/JSTARS.2018.2836155.

[17] D. A. Kumar, S. K. Meher, and K. P. Kumari, "Knowledge-based progressive granular neural networks for remote sensing image classification," *IEEE J Sel Top Appl Earth Obs Remote Sens*, vol. 10, no. 12, pp. 5201–5212, Dec. 2017, doi: 10.1109/JSTARS.2017.2743982.

[18] E. Pasolli, F. Melgani, D. Tuia, F. Pacifici, and W. J. Emery, "SVM active learning approach for image classification using spatial information," *IEEE Transactions on Geoscience and Remote Sensing*, vol. 52, no. 4, pp. 2217–2223, 2014, doi: 10.1109/TGRS.2013.2258676.

[19] D. Tuia, F. Ratle, F. Pacifici, M. F. Kanevski, and W. J. Emery, "Active learning methods for remote sensing image classification," *IEEE Transactions on Geoscience and Remote Sensing*, vol. 47, no. 7, pp. 2218–2232, Jul. 2009, doi: 10.1109/TGRS.2008.2010404.

[20] P. Mitra, B. Uma Shankar, and S. K. Pal, "Segmentation of multispectral remote sensing images using active support vector machines," *Pattern Recognit Lett*, vol. 25, no. 9, pp. 1067–1074, Jul. 2004, doi: 10.1016/J.PATREC.2004.03.004.

[21] G. Camps-Valls, T. v. Bandos Marsheva, and D. Zhou, "Semi-supervised graph-based hyperspectral image classification," *IEEE Transactions on Geoscience and Remote Sensing*, vol. 45, no. 10, pp. 3044–3054, Oct. 2007, doi: 10.1109/TGRS.2007.895416.

[22] J. Muñoz-Marí, F. Bovolo, L. Gómez-Chova, L. Bruzzone, and G. Camp-Valls, "Semisupervised one-class support vector machines for classification of remote sensing data," *IEEE Transactions on Geoscience and Remote Sensing*, vol. 48, no. 8, pp. 3188–3197, Aug. 2010, doi: 10.1109/TGRS.2010.2045764.

[23] F. de Morsier, D. Tuia, M. Borgeaud, V. Gass, and J. P. Thiran, "Semi-supervised novelty detection using SVM entire solution path," *IEEE Transactions on Geoscience and Remote Sensing*, vol. 51, no. 4, pp. 1939–1950, 2013, doi: 10.1109/TGRS.2012.2236683.

[24] L. Gómez-Chova, G. Camps-Valls, L. Bruzzone, and J. Calpe-Maravilla, "Mean map kernel methods for semisupervised cloud classification," *IEEE Transactions on Geoscience and Remote Sensing*, vol. 48, no. 1, pp. 207–220, Jan. 2010, doi: 10.1109/TGRS.2009.2026425.

[25] P. Mantero, G. Moser, and S. B. Serpico, "Partially supervised classification of remote sensing images through SVM-based probability density estimation," *IEEE Transactions on Geoscience and Remote Sensing*, vol. 43, no. 3, pp. 559–570, Mar. 2005, doi: 10.1109/TGRS.2004.842022.

[26] Y. Bazi and F. Melgani, "Semisupervised PSO-SVM regression for biophysical parameter estimation," *IEEE Transactions on Geoscience and Remote Sensing*, vol. 45, no. 6, pp. 1887–1895, Jun. 2007, doi: 10.1109/TGRS.2007.895845.

[27] N. Ghoggali and F. Melgani, "Genetic SVM approach to semisupervised multitemporal classification," *IEEE Geoscience and Remote Sensing Letters*, vol. 5, no. 2, pp. 212–216, Apr. 2008, doi: 10.1109/LGRS.2008.915600.

[28] N. Ghoggali, F. Melgani, and Y. Bazi, "A multiobjective genetic SVM approach for classification problems with limited training samples," *IEEE Transactions on Geoscience and Remote Sensing*, vol. 47, no. 6, pp. 1707–1718, Jun. 2009, doi: 10.1109/TGRS.2008.2007128.

[29] Y. Bazi and F. Melgani, "Toward an optimal SVM classification system for hyperspectral remote sensing images," *IEEE Transactions on Geoscience and Remote Sensing*, vol. 44, no. 11, pp. 3374–3385, Nov. 2006, doi: 10.1109/TGRS.2006.880628.

[30] C. E. Brodley and M. A. Friedl, "Decision tree classification of land cover from remotely sensed data," *Remote Sens Environ*, vol. 61, no. 3, pp. 399–409, Sep. 1997, doi: 10.1016/S0034-4257(97)00049-7.

[31] M. Xu, P. Watanachaturaporn, P. K. Varshney, and M. K. Arora, "Decision tree regression for soft classification of remote sensing data," *Remote Sens Environ*, vol. 97, no. 3, pp. 322–336, Aug. 2005, doi: 10.1016/J.RSE.2005.05.008.

[32] C. C. Yang *et al.*, "Application of decision tree technology for image classification using remote sensing data," *Agric Syst*, vol. 76, no. 3, pp. 1101–1117, Jun. 2003, doi: 10.1016/S0308-521X(02)00051-3.

[33] B. Feizizadeh and T. Blaschke, "Examining Urban heat Island relations to land use and air pollution: Multiple endmember spectral mixture analysis for thermal remote sensing," *IEEE J Sel Top Appl Earth Obs Remote Sens*, vol. 6, no. 3, pp. 1749–1756, 2013, doi: 10.1109/JSTARS.2013.2263425.

[34] A. Bateson and B. Curtiss, "A method for manual endmember selection and spectral unmixing," *Remote Sens Environ*, vol. 55, no. 3, pp. 229–243, Mar. 1996, doi: 10.1016/S0034-4257(95)00177-8.

[35] P. E. Dennison and D. A. Roberts, "Endmember selection for multiple endmember spectral mixture analysis using endmember average RMSE," *Remote Sens Environ*, vol. 87, no. 2–3, pp. 123–135, Oct. 2003, doi: 10.1016/S0034-4257(03)00135-4.

[36] D. R. Peddle, S. P. Brunke, and F. G. Hall, "A Comparison of Spectral Mixture Analysis and Ten Vegetation Indices for Estimating Boreal Forest Biophysical Information from Airborne Data," *https://doi.org/10.1080/07038992.2001.10854903*, vol. 27, no. 6, pp. 627–635, 2014, doi: 10.1080/07038992.2001.10854903.

International Journal of Engineering Research & Technology (IJERT)
ISSN: 2278-0181
Vol. 11 Issue 10, October-2022

[37] J. Yang, P. J. Weisberg, and N. A. Bristow, "Landsat remote sensing approaches for monitoring long-term tree cover dynamics in semi-arid woodlands: Comparison of vegetation indices and spectral mixture analysis," *Remote Sens Environ*, vol. 119, pp. 62–71, Apr. 2012, doi: 10.1016/J.RSE.2011.12.004.

[38] A. Kumar, A. Saha, and V. K. Dadhwal, "Some issues related with sub-pixel classification using HYSI data from IMS-1 satellite," *Journal of the Indian Society of Remote Sensing 2010 38:2*, vol. 38, no. 2, pp. 203–210, Dec. 2010, doi: 10.1007/S12524-010-0027-5.

[39] S. Yin, Y. Zhang, and S. Karim, "Large Scale Remote Sensing Image Segmentation Based on Fuzzy Region Competition and Gaussian Mixture Model," *IEEE Access*, vol. 6, pp. 26069–26080, May 2018, doi: 10.1109/ACCESS.2018.2834960.

[40] B. Choubin, K. Solaimani, M. Habibnejad Roshan, and A. Malekian, "Watershed classification by remote sensing indices: A fuzzy c-means clustering approach," *Journal of Mountain Science 2017 14:10*, vol. 14, no. 10, pp. 2053–2063, Oct. 2017, doi: 10.1007/S11629-017-4357-4.

[41] W. Liu, K. C. Seto, E. Y. Wu, S. Gopal, and C. E. Woodcock, "ART-MMAP: A neural network approach to subpixel classification," *IEEE Transactions on Geoscience and Remote Sensing*, vol. 42, no. 9, pp. 1976–1983, Sep. 2004, doi: 10.1109/TGRS.2004.831893.

[42] F. Bovolo, L. Bruzzone, and L. Carlin, "A novel technique for subpixel image classification based on support vector machine," *IEEE Transactions on Image Processing*, vol. 19, no. 11, pp. 2983–2999, Nov. 2010, doi: 10.1109/TIP.2010.2051632.

[43] R. Feng, Y. Zhong, X. Xu, and L. Zhang, "Adaptive Sparse Subpixel Mapping with a Total Variation Model for Remote Sensing Imagery," *IEEE Transactions on Geoscience and Remote Sensing*, vol. 54, no. 5, pp. 2855–2872, May 2016, doi: 10.1109/TGRS.2015.2506612.

[44] D. Liu and F. Xia, "Assessing object-based classification: advantages and limitations," *http://dx.doi.org/10.1080/01431161003743173*, vol. 1, no. 4, pp. 187–194, Dec. 2010, doi: 10.1080/01431161003743173.

[45] U. Benz and E. Pottier, "Object based analysis of polarimetric SAR data in alpha-entropy-anisotropy decomposition using fuzzy classification by eCognition," *International Geoscience and Remote Sensing Symposium (IGARSS)*, vol. 3, pp. 1427–1429, 2001, doi: 10.1109/IGARSS.2001.976867.

[46] M. E. Hodgson, J. R. Jensen, J. A. Tullis, K. D. Riordan, and C. M. Archer, "Synergistic Use of Lidar and Color Aerial Photography for Mapping Urban Parcel Imperviousness," *Photogramm Eng Remote Sensing*, vol. 69, no. 9, pp. 973–980, Sep. 2003, doi: 10.14358/PERS.69.9.973.

[47] L. Pierce, F. T. Ulaby, K. Sarabandi, and M. C. Dobson, "Knowledge-Based Classification of Polarimetric SAR Images," *IEEE Transactions on Geoscience and Remote Sensing*, vol. 32, no. 5, pp. 1081–1086, 1994, doi: 10.1109/36.312896.

[48] C. Kontoes, G. G. Wilkinson, A. Burrill, S. Goffredo, and J. Mégier, "An experimental system for the integration of GIS data in knowledge-based image analysis for remote sensing of agriculture," *http://dx.doi.org/10.1080/02693799308901955*, vol. 7, no. 3, pp. 247–262, 2007, doi: 10.1080/02693799308901955.

[49] J. Ton, J. Sticklen, and A. K. Jain, "Knowledge-Based Segmentation of Landsat Images," *IEEE Transactions on Geoscience and Remote Sensing*, vol. 29, no. 2, pp. 222–232, 1991, doi: 10.1109/36.73663.

[50] Y. Ban, H. Hu, and I. M. Rangel, "Fusion of Quickbird MS and RADARSAT SAR data for urban land-cover mapping: object-based and knowledge-based approach," *https://doi.org/10.1080/01431160903475415*, vol. 31, no. 6, pp. 1391–1410, 2010, doi: 10.1080/01431160903475415.

[51] S. W. Myint, P. Gober, A. Brazel, S. Grossman-Clarke, and Q. Weng, "Per-pixel vs. object-based classification of urban land cover extraction using high spatial resolution imagery," *Remote Sens Environ*, vol. 115, no. 5, pp. 1145–1161, May 2011, doi: 10.1016/J.RSE.2010.12.017.

[52] M. Li, S. Zang, B. Zhang, S. Li, and C. Wu, "A Review of Remote Sensing Image Classification Techniques: the Role of Spatio-contextual Information," *http://dx.doi.org/10.5721/EuJRS20144723*, vol. 47, no. 1, pp. 389–411, Jun. 2017, doi: 10.5721/EUJRS20144723.

[53] P. Du, J. Xia, W. Zhang, K. Tan, Y. Liu, and S. Liu, "Multiple Classifier System for Remote Sensing Image Classification: A Review," *Sensors 2012, Vol. 12, Pages 4764-4792*, vol. 12, no. 4, pp. 4764–4792, Apr. 2012, doi: 10.3390/S120404764.

[54] S. Fei *et al.*, "UAV-based multi-sensor data fusion and machine learning algorithm for yield prediction in wheat," *Precis Agric*, 2022, doi: 10.1007/S11119-022-09938-8.

[55] B. M. Steele, "Combining Multiple Classifiers: An Application Using Spatial and Remotely Sensed Information for Land Cover Type Mapping," *Remote Sens Environ*, vol. 74, no. 3, pp. 545–556, Dec. 2000, doi: 10.1016/S0034-4257(00)00145-0.

[56] P. Liu, K. K. R. Choo, L. Wang, and F. Huang, "SVM or deep learning? A comparative study on remote sensing image classification," *Soft Computing 2016 21:23*, vol. 21, no. 23, pp. 7053–7065, Jul. 2016, doi: 10.1007/S00500-016-2247-2.

[57] P. S. Sisodia, V. Tiwari, and A. Kumar, "A comparative analysis of remote sensing image classification techniques," *Proceedings of the 2014 International Conference on Advances in Computing, Communications and Informatics, ICACCI 2014*, pp. 1418–1421, Nov. 2014, doi: 10.1109/ICACCI.2014.6968245.

[58] X. Li, F. Ling, Y. Du, Q. Feng, and Y. Zhang, "A spatial–temporal Hopfield neural network approach for super-resolution land cover mapping with multi-temporal different resolution remotely sensed images," *ISPRS Journal of Photogrammetry and Remote Sensing*, vol. 93, pp. 76–87, Jul. 2014, doi: 10.1016/J.ISPRSJPRS.2014.03.013.

[59] "EarthExplorer." https://earthexplorer.usgs.gov/ (accessed Oct. 17, 2022).